ARTICLE

BIOTECHNOLOGY and BIOENGINEERING

Engineering of the Yeast Antioxidant Enzyme Mpr1 for Enhanced Activity and Stability

Kaoru Iinoya, Tetsuya Kotani, Yu Sasano, Hiroshi Takagi

Graduate School of Biological Sciences, Nara Institute of Science and Technology, 8916-5 Takayama, Ikoma, Nara 630-0192, Japan; telephone: +81-743-72-5420; fax: +81-743-72-5429; e-mail: hiro@bs.naist.jp

Received 3 November 2008; revision received 16 December 2008; accepted 29 December 2008

Published online 6 January 2009 in Wiley InterScience (www.interscience.wiley.com). DOI 10.1002/bit.22247

ABSTRACT: The budding yeast *Saccharomyces cerevisiae* Σ1278b has the *MPR1* gene, which confers resistance to the proline analogue azetidine-2-carboxylate (AZC). This gene encodes an *N*-acetyltransferase Mpr1 that detoxifies AZC, and the homologous genes have been found in many yeasts. Recently, we found that Mpr1 protects yeast cells by reducing the intracellular reactive oxygen species (ROS) levels under oxidative stresses, such as heat-shock, freezing, or ethanol treatment. Unlike the known antioxidant enzymes, Mpr1 is thought to acetylate toxic metabolite(s) involved in ROS generation via oxidative events. To improve the enzymatic functions of Mpr1, we applied PCR random mutagenesis to *MPR1*. The mutagenized plasmid library was introduced into the *S. cerevisiae* S288C strain lacking *MPR1*, and we successfully isolated two Mpr1 variants with higher AZC resistance (K63R and F65L/L117V). Interestingly, overexpression of the K63R variant was found to increase cell viability or decrease intracellular ROS levels after exposure to H_2O_2 or ethanol compared with the wild-type Mpr1. In vitro studies with the recombinant enzymes showed that the catalytic efficiency of the K63R variant for AZC and acetyl-CoA was higher than that of the wild-type Mpr1 and that the F65L mutation greatly enhanced the thermal stability. The mutational analysis and molecular modeling suggest that an α-helix containing Lys63 and Phe65 has important roles in the function of Mpr1. In addition, the wild-type and K63R variant Mpr1 reduced intracellular ROS levels under ethanol stress conditions on haploid sake yeast cells. These results suggest that engineering Mpr1 might be useful in breeding oxidative stress-tolerant yeast strains.

Biotechnol. Bioeng. 2009;103: 341–352.

KEYWORDS: *Saccharomyces cerevisiae*; antioxidant enzyme; Mpr1

Correspondence to: H. Takagi

Contract grant sponsor: Program for Promotion of Basic Research Activities for Innovative Biosciences (PROBRAIN)
Contract grant sponsor: Japan Society for the Promotion of Science
Contract grant number: 18380062
Contract grant sponsor: Nagase Science and Technology Foundation

Introduction

The *MPR1* gene (sigma 1278b gene for proline-analogue resistance) found in the budding yeast *Saccharomyces cerevisiae* Σ1278b encodes an *N*-acetyltransferase that detoxifies the proline analogue azetidine-2-carboxylate (AZC) (Shichiri et al., 2001; Takagi et al., 2000). We believe that the *MPR1*-encoded protein (Mpr1) converts AZC into *N*-acetyl AZC, and consequently *N*-acetyl AZC does not replace proline during the biosynthesis of proteins (Shichiri et al., 2001). Interestingly, *MPR1* was absent in the sequenced laboratory strain S288C, but the homologous genes including *Spa MPR1* (Kimura et al., 2002) and *ppr1*$^+$ (Nomura et al., 2003) have been identified in the genomes of *Saccharomyces paradoxus* and the fission yeast *Schizosaccharomyces pombe*, respectively. In a BLAST search of the protein database, we recently found that many yeasts and fungi have a DNA fragment homologous to *MPR1* (Du and Takagi, 2007). These results suggest that *MPR1* is widely present in yeast and fungus strains and is probably derived from a common ancestral gene.

However, it is unlikely that AZC is a natural substrate for Mpr1 because AZC occurs only in some plants (Fowden, 1956; Peterson and Fowden, 1963). Recently, we found that Mpr1 protects yeast cells by reducing the intracellular reactive oxygen species (ROS) levels under oxidative stresses, such as H_2O_2, heat-shock, freezing, or ethanol treatment (Du and Takagi, 2005, 2007; Nomura and Takagi, 2004). Genetic and enzymatic analyses showed that Mpr1 regulates the ROS level by acetylating proline catabolism intermediate Δ^1-pyrroline-5-carboxylate (P5C) and its equilibrium compound, glutamate-γ-semialdehyde (GSA) under P5C-induced oxidative stress (Nomura and Takagi, 2004). These results indicate that Mpr1 plays an important role in protecting yeast cells under oxidative stress by reducing the ROS level. Unlike many antioxidant enzymes that catalyze the direct decomposition of ROS, the antioxidant mechanism of Mpr1 is novel because this enzyme is thought to acetylate toxic metabolite(s) involved in ROS production, such as P5C, in response to an oxidative event.

Since *S. cerevisiae* cells are exposed to various oxidative stresses including freezing and ethanol treatment during fermentation processes, wild-type and its engineered Mpr1 proteins could be useful for breeding novel yeast strains that are tolerant to various oxidative stresses. Mpr1 is a member of the GCN5-related *N*-acetyltransferase (GNAT) superfamily, which is found in all kingdoms of life (Neuwald and Landsman, 1997; Takagi et al., 2000). These enzymes have four conserved sequence motifs (A–D) (Dyda et al., 2000; Neuwald and Landsman, 1997; Vetting et al., 2005). Motif A involved in acetyl-CoA binding contains a short consensus sequence, (Q/R)XXGX(G/A) (X denotes any amino acid residue) (Dutnall et al., 1998; Lu et al., 1996; Wolf et al., 1998). In the case of the Mpr1 sequence, the corresponding region consists of Arg145-Gly146-Gln147-Lys148-Val149-Gly150. The three-dimensional structure of Mpr1 has not yet been determined. Thus, in this study, we attempted to isolate the Mpr1 variants with improved enzymatic functions from the PCR-based mutagenized library and found that the K63R or F65L mutation enhanced the antioxidant activity or the thermal stability of Mpr1, respectively. We also tested the applicability of the K63R variant for breeding ethanol stress-tolerant sake yeast strains.

Materials and Methods

Strains and Plasmids

The *S. cerevisiae* strains CKY8 (*MATα leu2-3, 112 ura3-52 gal2*) and CKY263 (*MATa leu2-3, 112 ura3-52 GAL2*) with a S288C background (supplied by C. Kaiser) were used in this study. Strain XU-14 (*MATa ura3*) is a haploid derived from a sake yeast strain Kyokai no. 14 (K-14), which is a diploid prototroph (supplied by Y. Kubo). The 2μ-based high-copy-number plasmids pAD-MPR (Nomura et al., 2003) and pGAL-MPR, which contain the *S. cerecisiae LEU2* and *URA3* gene, were used to express *MPR1* under control of the *ADH1* and the *GAL1* promoter, respectively. Plasmid pGAL-MPR was constructed by cloning the 930 bp *Hin*dIII-*Mlu*I fragment of the *MPR1* gene from pMH1 (Takagi et al., 2000) into the *Hin*dIII-*Mlu*I site of pYES2 (Invitrogen, San Diego, CA).

Escherichia coli strain JM109 (*recA1 endA1 gryA96 thi-1 hsdR17 supE44 relA1* Δ(*lac-proAB*)/*F′* [*traD36 proAB*$^+$ *lacI*^{q} *lacZΔM15*]) was used as a host for plasmid construction and the *MPR1* gene expression. The isopropyl-β-D-thiogalactopyranoside (IPTG)-inducible vector TAGZyme (Qiagen, Hilden, Germany) with a sequence coding six-consecutive His residues at the 5′ end of the cloning sites was used to express *MPR1* in *E. coli* strain M15 [pREP4] (*lac ara gal mtl recA*$^+$ *uvr*$^+$ [*lacI kan*^{r}]).

Culture Media

The media used for growth of *S. cerevisiae* were a synthetic minimal medium SD (2% glucose, 0.67% bacto yeast nitrogen base without amino acids [Difco Laboratories, Detroit, MI]), SG (2% galactose, 0.67% bacto yeast nitrogen base without amino acids), and a nutrient medium YPD (2% glucose, 1% yeast extract, 2% peptone). When appropriate, required supplements were added to the media for auxotrophic strains. Yeast strains were also cultured on SG agar plates containing AZC (Sigma–Aldrich, St. Louis, MO). The *E. coli* recombinant strains were grown in Luria–Bartani (LB) complete medium (Sambrook and Russell, 2001) containing 50 μg/mL ampicillin or M9 minimal medium (Sambrook and Russell, 2001) plus 2% Casamino Acids (M9CA) containing 50 μg/mL ampicillin. If necessary, 2% agar was added to solidify the medium.

PCR Random Mutagenesis

The *MPR1* gene was amplified from pGAL-MPR by error-prone PCR with 5′-GCT CGA GAA GCT TCG AAT GC-3′ and 5′-CGA CGC GTC GTT ATT CGT TCT T-3′ (the underlining indicates the positions of a *Hin*dIII and *Mlu*I, respectively). Ten nanograms of pGAL-MPR DNA was added as a template to a solution containing 10 mM Tris–HCl (pH 9.0), 50 mM KCl, 1.5 mM $MgCl_2$, 0.1% Triton X-100, 0.05 mM dATP and dTTP, 0.16 mM dCTP and dGTP, 1.0 μM each of the two primers, and 0.25 μL of *Taq* DNA polymerase (5 U/μL) and enough distilled water to bring the total volume to 50 μL. Twenty-five cycles (94°C for 1 min, 55°C for 1 min, 72°C for 1 min) of PCR were carried out. The unique 930 bp amplified band was digested with *Hin*dIII and *Mlu*I, and ligated to the *Hin*dIII and *Mlu*I sites of pYES2. The ligated DNA was used to transform *E. coli* JM109 on LB solid medium containing ampicillin, and plasmid DNAs prepared from the ampicillin-resistant colonies (approximately 60,000) were used to isolate mutant Mpr1s as the mutagenized plasmid library.

Site-Directed Mutagenesis and Construction of Plasmids for Expressing the *Mpr1* Gene

For site-directed mutagenesis of the *MPR1* gene, an overlap extension method was performed (Ho et al., 1989). Plasmid pGAL-MPR was used as the template for the first round PCR with the complementary internal primers (Table I). In addition, S-*Hin*dIII+ (5′-GGC CAA GCT TAG ATG GAT GCG GAA TC-3′) and S-*Sac*I− (5′-CCC CGA GCT CTG TCT ATG ATT ATT CCA TGG-3′), or E-*Sac*I+ (5′-GGC CGA GCT CAG ATG GAT GCG GAA TC-3′) and E-*Hin*dIII− (5′-CCC CAA GCT TTT ATT CCA TGG AGA GGA ATT-3′) for the expression in *S. cerevisiae* or in *E. coli*, respectively, were used to amplify regions upstream and downstream of the target residues. The underlined sequences indicate the positions of the *Hin*dIII and *Sac*I restriction sites. Each group of two primary PCR products was purified with QIAquick Gel Extraction Kit (Qiagen) and mixed.

Table I. Primers used for site-directed mutagenesis.

Mutation	Primer DNA sequence[a]
K63R	5′-CTCATTAACTATCTTTTTAGATTGTTTAATTTGGAA-3′
	5′-TTCCAAATTAAACAATCTAAAAAGATAGTTAATGAG-3′
F65L	5′-ATTAACTATCTTTTTAAATTGCTTAATTTGGAAATTGAAAGTGGC-3′
	5′-GCCACTTTCAATTTCCAAATTAAGCAATTTAAAAAGATAGTTAAT-3′
L117V	5′-GACTGGAATTCAGTTCTCCTGGGCACATTCTACATCAAG-3′
	5′-CTTGATGTAGAATGTGCCCAGGAGAACTGAATTCCAGTC-3′
K63A	5′-CTCATTAACTATCTTTTTGCGTTGTTTAATTTGGAA-3′
	5′-TTCCAAATTAAACAACGCAAAAAGATAGTTAATGAG-3′
K63P	5′-CTCATTAACTATCTTTTTCCATTGTTTAATTTGGAA-3′
	5′-TTCCAAATTAAACAATGGAAAAAGATAGTTAATGAG-3′
K63I	5′-CTCATTAACTATCTTTTTATCTTGTTTAATTTGGAA-3′
	5′-TTCCAAATTAAACAAGATAAAAAGATAGTTAATGAG-3′
K63V	5′-CTCATTAACTATCTTTTTGTCTTGTTTAATTTGGAA-3′
	5′-TTCCAAATTAAACAAGACAAAAAGATAGTTAATGAG-3′
K63G	5′-CTCATTAACTATCTTTTTGGGTTGTTTAATTTGGAA-3′
	5′-TTCCAAATTAAACAACCCAAAAAGATAGTTAATGAG-3′
K63T	5′-CTCATTAACTATCTTTTTACGTTGTTTAATTTGGAA-3′
	5′-TTCCAAATTAAACAACGTAAAAAGATAGTTAATGAG-3′
K63S	5′-CTCATTAACTATCTTTTTTCCTTGTTTAATTTGGAA-3′
	5′-TTCCAAATTAAACAAGGAAAAAAGATAGTTAATGAG-3′
K63C	5′-CTCATTAACTATCTTTTTTGCTTGTTTAATTTGGAA3′
	5′-TTCCAAATTAAACAAGCAAAAAAGATAGTTAATGAG3′
K63Q	5′-CTCATTAACTATCTTTTTCAGTTGTTTAATTTGGAA-3′
	5′-TTCCAAATTAAACAACTGAAAAAGATAGTTAATGAG-3′
K63D	5′-CTCATTAACTATCTTTTTGAGTTGTTTAATTTGGAA-3′
	5′-TTCCAAATTAAACAAGTCAAAAAGATAGTTAATGAG-3′
K63F	5′-CTCATTAACTATCTTTTTTTTTTGTTTAATTTGGAA-3′
	5′-TTCCAAATTAAACAAAAAAAAAAAGATAGTTAATGAG-3′
K63Y	5′-CTCATTAACTATCTTTTTTAATTGTTTAATTTGGAA-3′
	5′-TTCCAAATTAAACAATTAAAAAAGATAGTTAATGAG-3′
F65W	5′-ATTAACTATCTTTTTAAATTGTGGAATTTGGAAATTGAAAGTGGC-3′
	5′-GCCACTTTCAATTTCCAAATTCCACAATTTAAAAAGATAGTTAAT-3′
F65S	5′-ATTAACTATCTTTTTAAATTGAGCAATTTGGAAATTGAAAGTGGC-3′
	5′-GCCACTTTCAATTTCCAAATTGCTCAATTTAAAAAGATAGTTAAT-3′
F65Q	5′-ATTAACTATCTTTTTAAATTGCAAAATTTGGAAATTGAAAGTGGC-3′
	5′-GCCACTTTCAATTTCCAAATTTTGCAATTTAAAAAGATAGTTAAT-3′
F65P	5′-ATTAACTATCTTTTTAAATTGCCCAATTTGGAAATTGAAAGTGGC-3′
	5′-GCCACTTTCAATTTCCAAATTGGGCAATTTAAAAAGATAGTTAAT3′
F65I	5′-ATTAACTATCTTTTTAAATTGATTAATTTGGAAATTGAAAGTGGC-3′
	5′-GCCACTTTCAATTTCCAAATTAATCAATTTAAAAAGATAGTTAAT-3′
F65G	5′-ATTAACTATCTTTTTAAATTGGGTAATTTGGAAATTGAAAGTGGC-3′
	5′-GCCACTTTCAATTTCCAAATTACCCAATTTAAAAAGATAGTTAAT-3′
F65D	5′-ATTAACTATCTTTTTAAATTGGACAATTTGGAAATTGAAAGTGGC-3′
	5′-GCCACTTTCAATTTCCAAATTGTCCAATTTAAAAAGATAGTTAAT-3′
F65R	5′-ATTAACTATCTTTTTAAATTGCGGAATTTGGAAATTGAAAGTGGC-3′
	5′-GCCACTTTCAATTTCCAAATTCCGCAATTTAAAAAGATAGTTAAT-3′
F65H	5′-ATTAACTATCTTTTTAAATTGCACAATTTGGAAATTGAAAGTGGC-3′
	5′-GCCACTTTCAATTTCCAAATTGTGCAATTTAAAAAGATAGTTAAT-3′

[a]The bases representing the nucleotide mutations are underlined.

For the expression in *S. cerevisiae* CKY8, the second PCR was performed with S-*Hin*dIII+ and S-*Sac*I−. The amplified 721 bp fragments were digested with *Hin*dIII and *Sac*I, ligated at the *Hin*dIII and *Sac*I sites of pAD4 and transformed into *E. coli* strain JM109. The nucleotide sequences were confirmed by DNA sequencing. For the expression in sake yeast XU-14, the 2.8 kb *Bam*HI fragment containing the *ADH1* promoter and *MPR1* of pAD-MPR or pAD-K63R was ligated into the *Bam*HI site of pYES2 to construct pADU-MPR or pADU-K63R, respectively. For the expression in *E. coli*, the mixtures were then used as templates for the second PCR with E-*Sac*I+ and E-*Hin*dIII−. The amplified 721 bp fragments were digested with *Sac*I and *Hin*dIII, ligated at the *Sac*I and *Hin*dIII sites of TAGZyme pQE2 and transformed into *E. coli* strain JM109.

Expression and Purification of the Recombinant Mpr1 Proteins

Each *E. coli* transformant prepared as described above was grown at 37°C in M9CA medium. When absorbance at

600 nm reached 0.7, IPTG was added to the culture medium to a final concentration of 0.1 mM to induce gene expression. After cultivation for 18 h at 18°C, the cells were harvested by centrifugation and suspended with ice-cold 50 mM NaH_2PO_4 buffer (pH 8.0) containing 300 mM NaCl, and the soluble fraction was prepared. The His-tagged fusion proteins in the soluble fraction were then purified using Ni–nitrilotriacetic acid–agarose (Qiagen) according to the procedure recommended by the supplier. Protein concentrations were determined using a Bio-Rad protein assay kit (Hercules, CA) with bovine serum albumin as the standard protein.

Western Blot Analysis

Total cellular proteins from extracts of *S. cerevisiae* and *E. coli* were separated on SDS–polyacrylamide gel electrophoresis and transferred onto Hybond-P (GE Healthcare, Piscataway, NJ). The wild-type and mutant proteins were detected by Western blot analysis with ECL Plus Western Blotting Detection System (GE Healthcare) using anti-Mpr1 antibody prepared previously (Shichiri et al., 2001).

Assays of Acetyltransferase Activity

The acetyltransferase activity was assayed at 30°C by monitoring the increase in 5-thio-2-nitrobenzoic acid (TNB) because of the reaction of CoA-SH with 5,5′-dithiobis(2-nitrobenzoic acid) (DTNB). The initial rate of the increase in absorbance at 412 nm of the reaction mixture (final volume, 1 mL) comprising 50 mM Tris–HCl buffer (pH 8.5), 5 mM AZC, 0.2 mM acetyl-CoA, 1 mM DTNB, and appropriate amount of enzyme was followed with a DU-640 spectrophotometer (Beckman Coulter, Fullerton, CA). The reaction rate was calculated with an extinction coefficient for TNB of 15,570 $M^{-1}\,cm^{-1}$. One unit is defined as the amount of enzyme catalyzing the formation of 1 μmol of TNB/min. The kinetic parameters K_m and k_{cat} were obtained from initial rate measurements by monitoring the absorbance increase at 412 nm with a DU-640 spectrophotometer (Beckman Coulter). When the apparent K_m value for AZC was determined, the AZC concentration was varied from 0.5 to 5 mM in the presence of a fixed concentration of acetyl-CoA (0.1 mM). When the apparent K_m value for acetyl-CoA was determined, the acetyl-CoA concentration was varied from 0.025 to 0.15 mM in the presence of a fixed concentration of AZC (5 mM).

Measurement of Intracellular Oxidation Level

The level of intracellular ROS induced in a cell during oxidative stress was measured with the oxidant-sensitive probe 2′, 7′-dichlorofluorescin diacetate (DCFDA) (Molecular Probes, Eugene, OR). This probe is trapped inside the cells after cleavage of the diacetate by an intracellular esterase (Royall and Ischiropoulos, 1993). It is then oxidized by radical species (mainly H_2O_2), a more fluorescent compound being produced (Tsuchiya and Suematsu, 1994).

In 500 mL flasks, the *S. cerevisiae* strains were grown to the exponentially growth phase in 200 mL of SD medium at 30°C with shaking. Yeast cells were harvested, resuspended in 100 mM potassium phosphate buffer (pH 7.4) (optical density at 600 nm of 1.0) containing 10 μM DCFDA, and incubated at 30°C for 15 min. The cells were incubated at 30°C with 2 mM H_2O_2 for 30 and 60 min or 18% ethanol for 2 and 4 h. After oxidative treatment, the cells were washed, resuspended in 500 μL of distilled water, and disrupted with glass beads in a Multi-Beads Shocker (MB601U, Yasui Kikai, Osaka, Japan) for 5 min. Cell extracts (50 μL) were mixed with 450 μL of distilled water, and the fluorescence was measured with $\lambda_{EX} = 490$ nm and $\lambda_{EM} = 524$ nm using a fluorescence spectrophotometer (F-7000; Hitachi, Tokyo, Japan). The value of $\lambda_{EM} = 524$ nm was normalized by protein in the mixture. Intensity of fluorescence of each strain before exposure to oxidative stress (0 min) was relatively taken as 100%.

Oxidative Stress Tolerance Test

Yeast cells were cultured to the exponential growth phase in SD medium at 30°C with shaking, washed with 0.9% NaCl, and concentrated to 2×10^6 cells/mL (optical density at 600 nm of 0.1) for H_2O_2 or ethanol treatment. Cells were then exposed to 2 mM H_2O_2 for 2 and 4 h or 18% ethanol for 4 and 8 h at 30°C. Before exposure to oxidative stress and at intervals thereafter, 0.1 mL of the culture was removed, diluted in distilled water, and aliquots were plated on YPD plates. After incubation at 30°C for 2 days, the survival rates were expressed as percentages, calculated as follows: (no. of colonies after exposure to oxidative stress)/(no. of colonies before exposure to oxidative stress) × 100.

Prediction of the Secondary and Tertiary Structures of Mpr1

The secondary structure prediction was performed by the program PredictProtein (http://www.predictprotein.org/). The three-dimensional structure was predicted using the computer program PHYRE (protein fold recognition server; http://www.sbg.bio.ic.ac.uk/phyre/), an automated system for construction of three-dimensional models of proteins based on homologues of known structures. The crystal structure of the *Bacillus subtilis* a hypothetical acetyltransferase [PDB code 1VHS (Badger et al., 2005)] belonging to the GNAT family was used as a template. Model was refined using the program Macromodel in the Maestro suite (Schrödinger, Portland, OR) and minimized using OPLS_2005 forcefield until an r.m.s.d. was <0.05 Å. The final model was visualized using Pymol version 0.99 (Delano Scientific, Palo Alto, CA).

Nucleotide Sequence Accession Numbers

The GenBank accession numbers for the *S. cerevisiae MPR1*, its homologues from the *S. paradoxus Spa MPR1* and the *S. pombe ppr1*$^{+}$ are AB031349, AB084520, and AB083128, respectively.

Results

The Mpr1 Variants With Higher AZC Resistance Were Isolated by PCR Random Mutagenesis

To improve the enzymatic properties of Mpr1, PCR random mutagenesis in *MPR1* was employed. Error-prone PCR was carried out as described in Experimental Procedures. In terms of industrial applications, H_2O_2 or ethanol tolerance is one of the most important traits for yeast cells. However, it appeared technically difficult for us to control the concentration of such volatile compounds on agar plates. We therefore tried to obtain the Mpr1 variants with enhanced tolerance to the non-volatile AZC instead of H_2O_2 or ethanol. The mutagenized plasmid library was introduced into *S. cerevisiae* CKY263 lacking *MPR1*, and transformants were selected on SG agar medium containing AZC (500 μg/mL). Transformants harboring pGAL-MPR and pYES2 were prepared as positive and negative controls, respectively. As a result, we obtained 29 AZC-resistant colonies capable of growing faster than the colonies expressing the wild-type Mpr1. Plasmids prepared from these colonies were then shuttled into *E. coli* JM109 and back into strain CKY263 to retest AZC resistance. Of the 29 plasmids, 2 were proved to confer higher AZC resistance, confirming that this phenotype was caused by a mutation(s) on the plasmid. The *MPR1* genes in the plasmids were sequenced, and two types of amino acid substitutions, Lys63Arg (K63R) (a single-base change from A to G at position 188) and Phe65Leu/Leu117Val (FL) (two single-base changes from T to C at positions 193 and 349), were identified.

The growth of yeast cells harboring the galactose-inducible expression plasmid (pGAL-MPR) is relatively slow in SG medium. Therefore, we constructed pAD4-based plasmids carrying the mutant *MPR1* genes with the constitutive *ADH1* promoter in SD medium and introduced the resultant plasmids into *S. cerevisiae* CKY8 lacking *MPR1*. As we expected, yeast cells expressing K63R or FL variant were more resistant to AZC than those expressing the wild-type Mpr1 (Fig. 1A). The vector pAD4-carrying cells failed to grow on the plate. These results suggest that two Mpr1 variants have an increased activity or stability compared to the wild-type enzyme.

To investigate the degree to which each substitution in the FL variant having double amino acid substitutions contributed to enzymatic function, two pAD4-based plasmids carrying the single mutation F65L or L117V were constructed by site-directed mutagenesis. In addition, three plasmids carrying the double mutations Lys63Arg/Phe65-Leu (KF) and Lys63Arg/Leu117Val (KL), and the triple mutations Lys63Arg/Phe65Leu/Leu117Val (KFL) were constructed by site-directed mutagenesis. The resultant plasmids were introduced into strain CKY8. As shown in Figure 1B, the levels of *MPR1* gene expression were almost the same for all mutants, based on densitometric estimates of the amounts of accumulated Mpr1 in the soluble fraction by Western blot analysis.

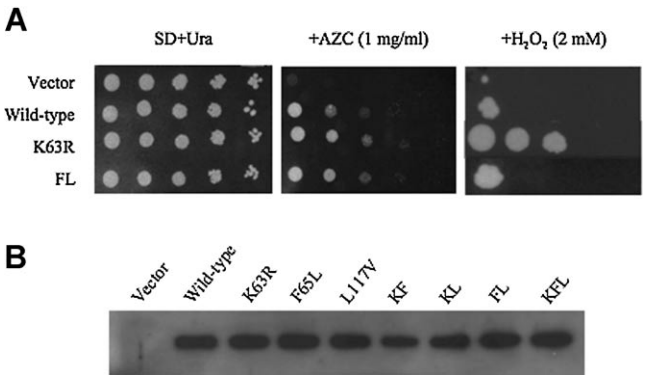

Figure 1. Isolation and expression of the wild-type and variant Mpr1 proteins. **A**: Growth phenotype of *S. cerevisiae* CKY8 transformants. After cultivation in liquid SD + Ura medium at 30°C for 48 h, approximately 10^6 cells carrying only the vector, the wild-type, the K63R mutant, the F65L/L117V mutant (FL) *MPR1* gene, and serial dilutions of 10^{-1} to 10^{-4} (from left to right) were spotted and incubated on SD + Ura agar medium containing 1 mg/mL AZC or 2 mM H_2O_2 at 30°C for 3 or 6 days, respectively. **B**: Western blot analysis of the cell extracts of *S. cerevisiae* CKY8 transformants. Total cellular proteins (10 μg) were subjected to a 15% polyacrylamide gel and were detected by using an anti-Mpr1 polyclonal antibody.

Yeast Cells Expressing the K63R Variant Showed Enhanced Oxidative-Stress Tolerance

We previously found that Mpr1 is involved in yeast cell growth in the presence of oxidative stress, including H_2O_2, heat-shock, freezing, or ethanol treatment (Du and Takagi, 2005; Du and Takagi, 2007; Nomura and Takagi, 2004). Interestingly, when yeast cells on SD medium were exposed to the oxidative stress of H_2O_2 (Fig. 1A) or heat-shock (data not shown), cells overexpressing the K63R variant showed a much greater tolerance than those overexpressing the wild-type Mpr1. However, the FL mutation did not enhance stress resistance to H_2O_2 and heat-shock (data not shown).

Next, we determined cell viability of transformants exposed to H_2O_2 in a liquid medium (Fig. 2A). When high-copy-number plasmid pAD-MPR harboring the wild-type *MPR1* was introduced into strain CKY8, the transformant showed a twofold higher survival rate after exposure to 2 mM H_2O_2 for 2 h as compared with that of CKY8 carrying only the vector. It is worth noting that in the K63R variant an approximately twofold increase was observed compared with the survival rate of the wild-type Mpr1. However, there were no significant differences in cell viability between yeast cells expressing the wild-type, F65L,

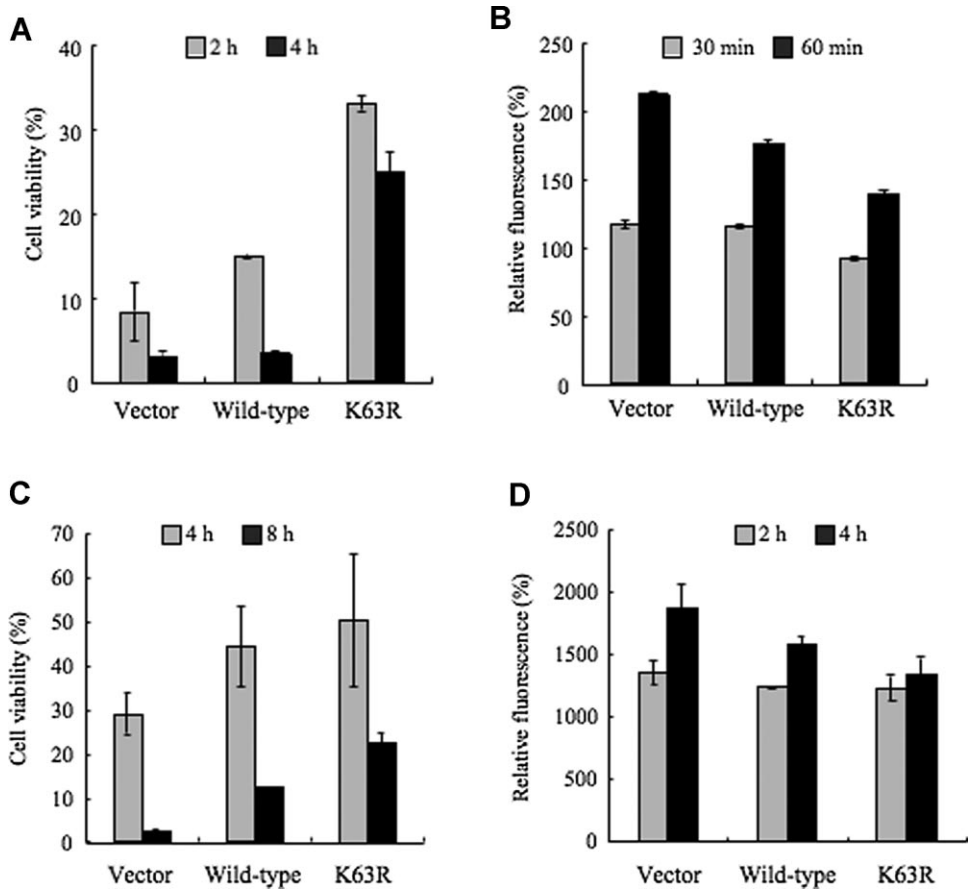

Figure 2. Effect of the wild-type and K63R variant Mpr1 proteins on yeast cells under oxidative stress conditions. **A**,**C**: Cell viability of *S. cerevisiae* CKY8 transformants. The survival rate of each strain in SD + Ura liquid medium was measured after incubation with 2 mM H_2O_2 at 30°C for 2 and 4 h (A) or with 18% ethanol at 30°C for 4 and 8 h (C). **B**,**D**: Intracellular oxidation level of *S. cerevisiae* CKY8 transformants. The intensity of fluorescence of each strain in SD + Ura liquid medium was measured after incubation with 2 mM H_2O_2 at 30°C for 30 and 60 min (B) or with 18% ethanol at 30°C for 2 and 4 h (D). Intensity of fluorescence of each strain before exposure to oxidative stress (0 min) was relatively taken as 100%. Results indicate the mean and standard deviation from three independent experiments.

L117V, KF, KL, or FL variant Mpr1, although the cells were more resistant to H_2O_2 than cells carrying only the vector (data not shown). We did not test the viability of cells expressing the triple mutant KFL due to a marked decrease of catalytic activity and stability as described in detail below. These results showed that the K63R mutation in Mpr1 is effective for yeast protection to H_2O_2.

The K63R Variant Further Reduce the Intracellular ROS Levels Under Oxidative Stress

Mpr1 was found to protect yeast cells by reducing the intracellular ROS levels under oxidative stress (Du and Takagi, 2005, 2007; Nomura and Takagi, 2004). We therefore examined the effect of mutant Mpr1 proteins on intracellular ROS levels generated by oxidative stress (Fig. 2B). We first measured the relative fluorescence at the same time for cell viability, but the reproducible values could not be obtained because dead cells may interfere with the accurate measurement of the intracellular fluorescence. During exposure to 2 mM H_2O_2 for up to 1 h, which does not immediately cause cell death, the ROS level in strain CKY8 overexpressing the wild-type Mpr1 continued to decrease and was approximately 20% lower than that in CKY8 cells carrying only the vector. Corresponding to the data of survival rates, the oxidation level was further reduced by 20–22% in the K63R variant. However, when the KF, KL, or FL variant was overexpresed in CKY8 cells, the intracellular ROS levels were virtually unchanged from those of the wild-type Mpr1. Contrary to our expectations, the mean fluorescence in the cells overexpressing the F65L or L117V variant was significantly lower than that in the cells overexpressing the wild-type Mpr1, although the survival rates in these cells were close to that in cells with the wild-type Mpr1 (data not shown). These results indicate that overexpression of the K63R variant led to a decrease in ROS levels and an increase in cell viability during H_2O_2 treatment, compared with expression of the wild-type Mpr1.

Based on recent reports that ethanol stress represents toxicity through intracellular ROS generation (Costa et al., 1997; Du and Takagi, 2007), we examined the effect of the

K63R variant in pAD4-based plasmids under ethanol stress conditions. *S. cerevisiae* cells overexpressing the K63R variant showed approximately 1.8-fold higher viability compared with cells overexpressing the wild-type Mpr1 after exposure to 18% ethanol for 8 h (Fig. 2C). When relative fluorescence data were measured after exposure to ethanol for 8 h, the values were very unreliable probably due to serious cell damage caused by ethanol. After incubation with ethanol for 4 h, an approximately 15% decrease of the ROS level was also observed in cells overexpressing the K63R variant as compared with cells overexpressing the wild-type Mpr1 (Fig. 2D). These results showed that the antioxidant activity in response to H_2O_2 or ethanol treatment was improved in the K63R variant.

Purification and Characterization of the Mpr1 Variants From *E. coli*

His-tagged wild-type and variant Mpr1 proteins were purified from the soluble fractions by a one-step procedure. Sodium dodecyl sulfate–polyacrylamide gel electrophoresis analysis revealed that all recombinant Mpr1 proteins were purified to give a single band, corresponding to 27.9 kDa (data not shown). To further analyze the characteristics of various Mpr1 proteins, Eadie–Hofstee plots were used to estimate the K_m and k_{cat} values for AZC and acetyl-CoA, and the results are summarized in Table II. The plots of Mpr1 activity versus AZC or acetyl-CoA concentration displayed typical Michaelis–Menten kinetics. Interestingly, all three of the single mutants were found to have an increased catalytic efficiency (k_{cat}/K_m value) compared to the wild-type Mpr1. A significant 1.5- to 2-fold increase in the values for both substrates was seen in the L117V mutant. The K63R variant also exhibited a 14% and 32% increase in the values for AZC and acetyl-CoA, respectively, which was predominantly caused by a lower K_m. The F65L substitution caused a prominent twofold increase in the values due to a lower K_m for AZC. However, the three double variants (KF, KL, and FL) showed a catalytic efficiency equivalent to that of the wild-type enzyme. It is noteworthy that the KFL mutation resulted in a significant decrease in the k_{cat}/K_m values, mainly due to the lower k_{cat} values for both substrates.

To determine the stability of these enzymes, the rate of thermal inactivation was measured at 50°C (Table II). Interestingly, the half-life ($t_{1/2}$) of the F65L, KF, and FL variants with the common F65L mutation was found to be four to six times longer than that of the wild-type enzyme. However, the half-life of the KFL mutant was 48% of that of the wild-type enzyme. The K63R or L117V mutation exhibited a half-life nearly equivalent to that of the wild-type enzyme. These results with the recombinant enzymes showed that the catalytic efficiency of the K63R and L117V variants was higher than that of the wild-type enzyme and that the F65L mutation greatly enhanced the thermal stability of Mpr1.

Functional Analysis of Lys63 and Phe65 in the Mpr1 Protein

Next, we examined which amino acid residues are involved in the activity and stability of Mpr1. Since there are no data on the three-dimensional structure, we first predicted the secondary structure of Mpr1 by the method of Chou and Fasman (1978). The predicted structure consisted of five α-helices and seven β-sheets seen in Mpr1. Two mutation sites, Lys63 and Phe65, might be located in a α-helix, which is made up of residues 55–70 (Fig. 3A). It is noteworthy that Lys63 and Phe65 are non-conserved residues among the Mpr1 homologues and GNAT superfamily and that the function is unknown. In contrast, Leu117 was found within the conserved regional motif D in the NAT superfamily (Neuwald and Landsman, 1997) (Fig. 3A). The three-dimensional localization of these mutation sites in Mpr1 was predicted by the method of homology modeling (Fig. 3B). Mpr1 shares less than 25% overall primary sequence identity with other GNAT structure-determined proteins (Angus-Hill et al., 1999; Badger et al., 2005; Hickman et al., 1999;

Table II. Kinetic constants and thermal stability of the wild-type and variant Mpr1 proteins.

	AZC			Acetyl-CoA			
Enzyme	k_m (mM)	k_{cat} (s^{-1})	k_{cat}/K_m ($s^{-1}mM^{-1}$)	K_m (μM)	k_{cat} (s^{-1})	k_{cat}/K_m ($s^{-1}\mu M^{-1}$)	Half-life at 50°C (min)
Wild-type	1.6 ± 0.09	36 ± 1.5	22 ± 1.3	13 ± 1.5	31 ± 0.63	2.5 ± 0.26	8.2
K63R	1.2 ± 0.17	31 ± 1.4	25 ± 2.6	8.0 ± 2.8	27 ± 0.94	3.3 ± 1.1	8.3
F65L	0.70 ± 0.15	31 ± 1.3	46 ± 8.6	10 ± 1.5	31 ± 0.61	2.9 ± 0.38	43
L117V	1.4 ± 0.13	48 ± 1.6	33 ± 2.6	7.6 ± 2.0	38 ± 0.74	5.0 ± 1.2	7.3
KF	2.2 ± 0.40	51 ± 3.8	23 ± 2.9	19 ± 2.2	42 ± 1.7	2.2 ± 0.18	52
KL	1.7 ± 0.18	46 ± 1.3	27 ± 2.2	11 ± 3.5	38 ± 1.6	3.7 ± 1.2	11
FL	1.8 ± 0.19	38 ± 2.2	21 ± 1.6	13 ± 1.7	31 ± 0.17	2.3 ± 0.32	34
KFL	1.2 ± 0.11	11 ± 0.54	9.5 ± 0.45	4.9 ± 3.3	9.1 ± 0.43	2.3 ± 1.1	3.9
K63P	1.6 ± 0.25	19 ± 0.45	12 ± 2.3	19 ± 4.1	15 ± 1.1	0.80 ± 0.10	3.1
F65G	3.3 ± 0.35	16 ± 0.30	4.7 ± 0.45	140 ± 11	17 ± 0.33	0.12 ± 0.01	2.3

Assays were performed in 50 mM Tris–HCl (pH 8.5) at 30°C using 0.6–1.0 μg of purified enzyme. Half-life was determined from the semi-log plot of $\log_{10}$ [residual activity] versus time. The values for kinetic constants are means ± SD from three independent experiments. The variations in the values for thermal stability were less than 5%.

Figure 3. Features of the Mpr1 protein. **A**: Comparison of the amino acid sequence of *S. cerevisiae* Mpr1 (MPR1) with that of *S. pombe* Ppr1 (ppr1) and S. *paradoxus* Spa Mpr1 (Spa MPR1). Identical and similar amino acids in two proteins are shown as bold letters. Red cylinders and yellow arrows above the sequences depict predicted α-helices and β-sheets, respectively. Dashes indicate the absence of corresponding amino acid residues at those positions. **B**: Predicted tertiary structure obtained by use of the computer program PHYRE. Predicted α-helices and β-sheets are shown in red and yellow, respectively. The *MPR1* mutation sites (Lys63, Phe65, and Leu117) are shown in gray. The Arg145 and Tyr166 residues, which are critical for the Mpr1 function (Kotani and Takagi, 2008), are also shown in gray.

Peneff et al., 2001; Poux et al., 2002; Vetting et al., 2002; Wolf et al., 2002). Thus, as a template for the modeling of Mpr1, we used the crystal structure of the *B. subtilis* hypothetical acetyltransferase (Vetting et al., 2005) belonging to the GNAT family. Within the overall region, the predicted amino acid sequence of this protein showed 21% identity to that of Mpr1. In a search of Protein Data Bank (http://www.rcsb.org/pdb/home/home.do), which is a repository for three-dimensional structural data of proteins obtained by X-ray crystallography, we unfortunately cannot find any proteins with more than 21% identity to that of Mpr1. The X-ray crystallographic study of Mpr1 is in progress and the three-dimensional structure will be published elsewhere. As seen in the predicted secondary structure, Lys63 and Phe65 were found in a α-helix, one of the five helices.

Our results suggest that Lys63 and Phe65 located in a putative α-helix have an important role in the catalysis and stability of Mpr1. To investigate the role of these residues in the Mpr1 function, additional mutations of Lys63 and Phe65 were performed using site-directed mutagenesis; namely, Lys63 was changed to 12 amino acids Ala, Pro, Ile, Val, Gly, Thr, Ser, Cys, Gln, Asp, Phe, and Tyr with different charges, hydrophobicities, and side chain volumes. Similarly, eight amino acids, Trp, Ser, Gln, Pro, Ile, Gly, Asp, Arg, and His, were introduced at position 65. These mutated *MPR1* genes were introduced into *E. coli* JM109 cells. The transformants possessing various mutant Mpr1 proteins were cultivated on AZC-containing M9 agar plates (Fig. 4A). *E. coli* cells expressing the K63P and K63Y variants were sensitive to AZC as well as those carrying only the vector, but the growth of other Lys63 variants was nearly equivalent to that of the wild-type Mpr1 on AZC-containing medium. In contrast, most of the Phe65 variants exhibited a growth defect in AZC. Only the F65W mutation conferred AZC resistance as well as wild-type Mpr1. These results suggest that most of the substitutions at position 63 have little influence on the function of Mpr1. Meanwhile, Phe65 is likely to be a crucial residue for the Mpr1 activity.

To further study the effects of these residues on the Mpr1 function, Western blot analysis was performed (Fig. 4B). We found that the amounts of the F65P and F65R variants were considerably lower than that of wild-type Mpr1. Because the levels of gene expression should be the same, this result suggests that these variants are very unstable. The instability of these variants might lead to the susceptibility to cellular protease(s) in *E. coli*. Strangely, the presence of Mpr1 could not be detected in cells overexpressing the K63Y and F65I variants. These recombinant cells might be sensitive to AZC due to unknown failure of the gene expression. We also examined the kinetic properties of the purified K63P and F65G variants (Table II). The k_{cat}/K_m values of these variants for both substrates were lower than that of wild-type Mpr1. In addition to a reduction of catalytic activity, the thermal stability of two mutants fell to about 30% of that of the wild-type enzyme (Table II). In general, Pro and Gly residues tend to break a α-helix in the protein. These results strongly suggest that a α-helix containing Lys63 and Phe65 is important for the function of Mpr1.

Effect of Mpr1 on Sake Yeast Cells Under Ethanol Stress Conditions

It is intriguing to evaluate the possibility of Mpr1 for breeding stress-resistant yeast strains. During the fermentation of sake, a traditional Japanese alcoholic beverage, yeast cells are exposed to high concentrations of ethanol [~20%

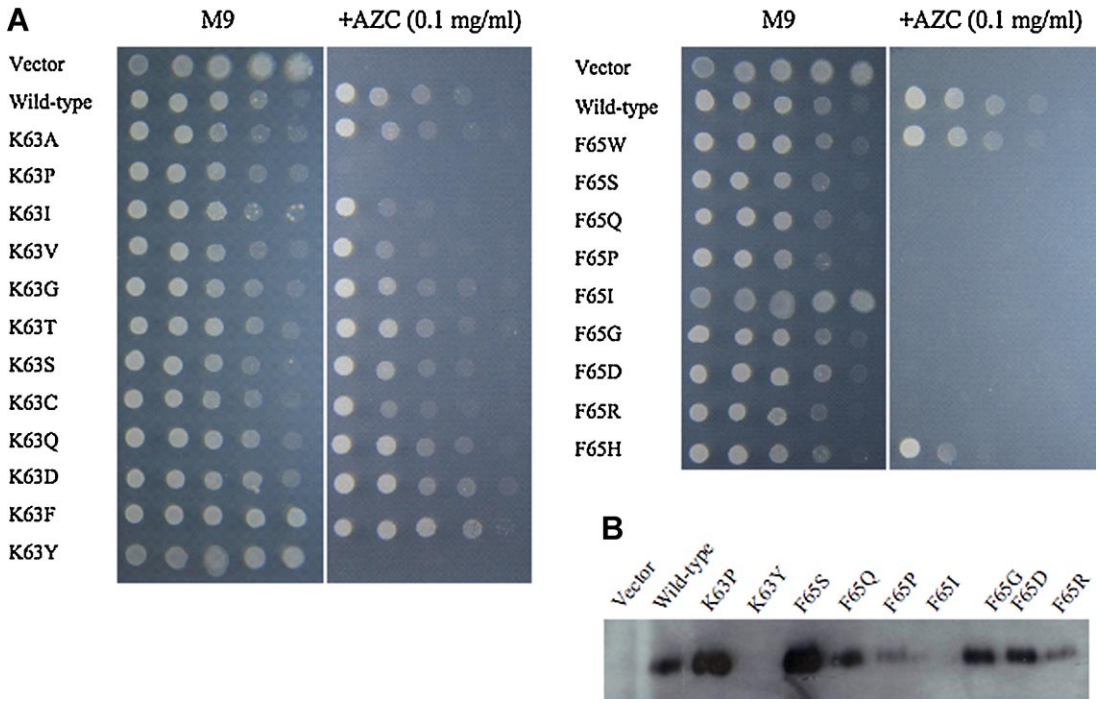

Figure 4. Effect of the Lys63 and Phe65 mutations on the Mpr1 function. A: Growth phenotype of *E. coli* JM109 transformants. After cultivation in liquid M9CA medium containing 50 μg/mL ampicillin at 37°C for 20 h, approximately 10^6 cells carrying each *MPR1* gene and serial dilutions of 10^{-1} to 10^{-4} (from left to right) were spotted and incubated on M9 agar medium containing 0.1 mM IPTG and 50 μg/mL ampicillin in the absence and presence of 0.1 mg/mL AZC at 37°C for 1 day. **B**: Western blot analysis of the cell extracts of *E. coli* JM109 transformants. Total cellular proteins (10 μg) were subjected to a 15% polyacrylamide gel and were detected by using an anti-Mpr1 polyclonal antibody. [Color figure can be seen in the online version of this article, available at www.interscience.wiley.com.]

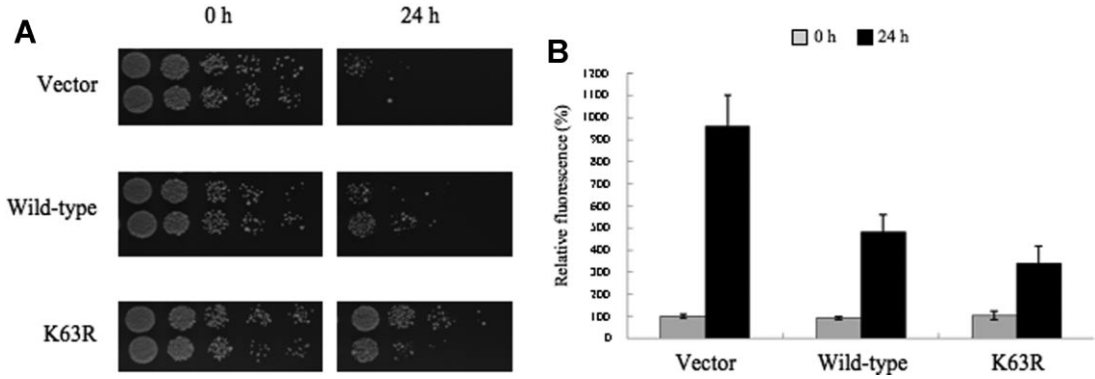

Figure 5. Effect of the wild-type and K63R variant Mpr1 proteins on sake yeast cells under ethanol stress conditions. A: Growth phenotype of sake strain XU-14 transformants. After cultivation in 100 mM potassium phosphate buffer (pH 7.5) containing 9% ethanol at 30°C for 0 and 24 h, approximately 10^6 cells carrying only the vector, the wild-type, the K63R mutant *MPR1* gene, and serial dilutions of 10^{-1} to 10^{-4} (from left to right) were spotted and incubated on YPD agar medium at 30°C for 2 days. B: Intracellular oxidation level of sake strain XU-14 transformants. The intensity of fluorescence of each strain in 100 mM potassium phosphate buffer (pH 7.5) was measured after incubation with 9% ethanol at 30°C for 0 and 24 h. The intensity of fluorescence of strain XU14 carrying pYES2 before exposure to ethanol stress (0 h) was relatively taken as 100%. Results indicate the mean and standard deviation from three independent experiments.

(v/v)]. It should be noted that the *MPR1* gene is missing in sake yeast strains (Takagi et al., unpublished work). Therefore, we constructed haploid sake yeast strains that overexpress the wild-type or K63R variant Mpr1 by introducing high-copy-number plasmid pADU-MPR or pADU-K63R, respectively. After exposure to 9% ethanol for 24 h, it appears that the wild-type or K63R variant Mpr1 conferred ethanol resistance to sake yeast cells slightly higher than those carrying only the vector (Fig. 5A). We also found the ROS level in strain XU-14 harboring the wild-type *MPR1* was about 50% lower than that in XU-14 cells carrying only the vector. The oxidation level was further reduced by approximately 30% in the K63 variant (Fig. 5B). These results showed that the expression of Mpr1 could reduce the ROS level in sake yeast cells.

Discussion

In this study, we newly isolated and analyzed Mpr1 variants with enhanced enzyme functions. Overexpression of the K63R variant was found to increase cell viability or decrease intracellular ROS levels after exposure to H_2O_2 or ethanol compared with the wild-type Mpr1 (Fig. 2). With respect to kinetic parameters (Table II), it is apparent that the K63R mutation resulted in an augmentation in the k_{cat}/K_m values for AZC and acetyl-CoA, but this is not a very dramatic increase compared with that of the antioxidant activity. In contrast, the antioxidant activity of the other two single mutants (F65L and L117V) was not enhanced, although the catalytic efficiency for AZC was significantly improved. As we previously reported (Kotani and Takagi, 2008; Nomura et al., 2003), the wild-type Mpr1 has a high affinity for acetyl-CoA (K_m: approx. 10 μM), and therefore, a lower K_m value for acetyl-CoA would not influence the antioxidant activity. It is probable that the K63R variant resulted in a marked preference for toxic intermediate(s) involved in ROS generation, such as P5C (Nomura and Takagi, 2004), rather than AZC. In the F65L and L117V mutants, the affinity for the substrate(s) under oxidative stress may remain unaltered. The mutations obtained here would influence on the acetylation of P5C, which is a cellular substrate of Mpr1. However, P5C is not available now, so we have not studied yet. We unexpectedly found that the triple mutant (KFL) decreased the enzymatic functions, suggesting that three cumulative amino acid substitutions might cause an unfavorable structural change in Mpr1.

As shown in Figure 2, however, there is not a clear correlation between relative fluorescence and cell viability. Our results could reflect the influence of factors other than Mpr1 on H_2O_2 or ethanol tolerance. DNA microarray analysis revealed that a set of genes involved in metabolism of stress protectants (glycerol, trehalose, proline, and glutathione, etc.) and antioxidant enzyme genes (catalase, superoxide dismutase, and thioredoxin peroxidase, etc.) do not respond to overexpression of *MPR1* (Takagi et al., unpublished work). It may be possible that Mpr1 acts as a backup system for oxidative stress-induced antioxidant enzyme genes. Regarding ethanol, direct damage to the protein structure and to membrane permeability, rather than the secondary effect of intracellular ROS generation, causes serious injury to cells during exposure to ethanol. A combination of stress protectants, for example, glycerol, trehalose, glutathione, and proline, might result in an even higher resistance to these stresses.

The replacement of Phe65 by Leu greatly enhanced the thermal stability of Mpr1 (Table II). With regard to the stability, we also evaluated the Mpr1 proteins for resistance to inactivation by H_2O_2. In general, many proteins and enzymes are easily inactivated by H_2O_2. For example, subtilisin from *Bacillus amyloliquefaciens* was rapidly inactivated by 0.1 M H_2O_2 ($t_{1/2} = \sim 2.5$ min) (Estell et al.,

1985), and manganese peroxidase from *Phanerochaete chrysosporium* has no detectable activity in the presence of 1.0 mM H_2O_2 (Miyazaki-Imamura et al., 2003). However, a surprising feature is that the Mpr1 proteins are very stable to H_2O_2 even in the presence of higher concentrations of 0.5 and 1.0 M. The residual activity of the wild-type Mpr1 was 73% after incubation with 1.0 M H_2O_2 at 25°C for 5 min. All of the Mpr1 variants (K63R, F65L, L117V, KF, KL, and FL) were also little affected by 1.0 M H_2O_2; the activities remaining were 73–82%. These results suggest that Mpr1 shows extremely higher stability to H_2O_2 than the other proteins. We now consider two possible explanations for this finding: (i) Mpr1 contains no Met residues in or around the active site that lead to oxidative inactivation that correlates directly with the production of methionine sulfoxide, and (ii) the dimerization of Mpr1 (Nomura et al., 2003) includes an intermolecular disulfide bond occurring between the surface Cys residues at positions 130 and 134, and this bond inhibits the oxidative formation of cysteine sulfonate, which may cause protein inactivation. Therefore, the F65L mutation would be only effective for improving the stability at the elevated temperature.

Our results showed that Lys63 and Phe65 are critical residues for the Mpr1 functions. When Lys63 is changed to Arg, a computational modeling suggested that an increase in the number of hydrogen bonds with the substrates (AZC and acetyl-CoA) might occur (Fig. 3B). In contrast, a side chain of Phe65 is likely to interact with a side chain(s) of several residues including the conserved Arg145 involved in AZC and acetyl-CoA binding (Kotani and Takagi, 2008; Shichiri et al., 2001). The Phe-to-Leu substitution at position 65 may cause the structural stability of the whole protein. The fact that the Leu117Val variant has higher catalytic efficiency than the wild-type Mpr1 may be due to its shorter side chain, which would decrease the steric hindrance at the substrate-binding pocket. Additional site-directed mutagenesis at Lys63 and Phe65 yielded different results (Fig. 4). The substitutions of Lys63 with most of amino acid residues conferred AZC resistance to yeast cells even with the oppositely charged Asp. It is reasonable to assume that Pro or Tyr at position 63 would severely impair the whole structure of Mpr1 because these residues are capable of breaking a α-helical structure. In contrast, the amino acid substitutions at position 65, except for Trp and His, might have led to the drastic structural change around the active site that resulted in a yeast growth defect to AZC. A possible reason for the structural change is that a decrease in the number of hydrogen bonds and/or steric hindrance between the Arg145 and the 65th residue would occur when an amino acid with different hydrophobicity and a side chain was introduced at position 65.

As shown in Figure 4A, *E. coli* cells expressing the K63P, F65G, or F65P variant showed AZC sensitivity at 37°C on M9 agar plates. This is probably because the structural change caused by amino acid substitution in the α-helix would lead to destabilization of the Mpr1 molecule at 37°C. It seems likely that lower temperature inhibits the denaturation or degradation of the labile proteins in *E. coli* cells. As we would expect, when cultivated at lower temperature of 18°C, transformants expressing the K63P or F65G variant could grow on the AZC-containing plates at a rate equivalent to that of cells expressing the wild-type Mpr1 (data not shown). These results suggest that the K63P and F65G variants have sufficient catalytic activity to acetylate AZC at low temperature, and that the predicted α-helix containing Lys63 and Phe65 may stabilize or assist the correct folding of the Mpr1 protein. Due to the lethal structural change caused by amino acid substitution, the F65P variant might be fully inactivated even at low temperature.

In terms of biotechnological applications, Mpr1 was found to reduce intracellular ROS level of sake yeast cells, although there is not a clear correlation with ethanol tolerance (Fig. 5). It is probable that the genetic backgrounds of the *S. cerevisiae* strains used result in the differences in ethanol tolerance. Interestingly, we found that a sake strain showed a poor growth on agar plates containing 9% ethanol, although a laboratory strain can grow on the same medium (data not shown). Also, a sake strain showed approximately 30% increase in the ROS level after exposure to 9% ethanol for 24 h, relative to that of a laboratory strain (Du and Takagi, 2007). These results suggest that a sake strain is sensitive to the acute ethanol stress than a laboratory strain, but can adapt to an increasing concentration of ethanol under sake brewing conditions (Wu et al., 2006). Our results also could reflect the influence of factors other than Mpr1 on ethanol tolerance. Costa et al. (1997) have reported that mitochondrial superoxide dismutase (encoded by *SOD2*) is essential for ethanol tolerance in yeast cells. Ethanol toxicity is correlated with ROS production in the mitochondria (Costa et al., 1997), which has been suggested as a target for ethanol damage (Aguilera and Benitez, 1985). However, the physical damage caused by protein denaturation and membrane disorder (Casey and Ingledew, 1986; Piper, 1995), rather than the secondary effect of intracellular ROS generation, causes serious injury to yeast cells during exposure to ethanol. Thus, increasing ethanol tolerance in yeast cells should improve the fermentation performance or simplify the fermentation process for the production of alcoholic beverages or bioethanol. Hence, the antioxidant Mpr1 could deserve further investigations as a potential stress protectant to improve ethanol tolerance in sake yeast strains.

We thank A. Sekiguchi, X. Du (Fukui Prefectural University, Fukui, Japan) and T. Yin (University of Minnesota, St. Paul, MN) for their technical assistances, and C. Kaiser (Massachusetts Institute of Technology, Cambridge, MA) and Y. Kubo (Fukui Prefectural Food Processing Research Institute, Fukui, Japan) for providing yeast strains. This work was supported by a grant for the Program for Promotion of Basic Research Activities for Innovative Biosciences (PROBRAIN), by a Grant-in-Aid for Scientific Research (B) (18380062) from Japan Society for the Promotion of Science, and by Nagase Science and Technology Foundation to H.T.

References

Aguilera A, Benitez T. 1985. Role of mitochondria in ethanol tolerance of *Saccharomyces cerevisiae*. Arch Microbiol 142:389–392.

Angus-Hill ML, Dutnall RN, Tafrov ST, Sternglanz R, Ramakrishnan V. 1999. Crystal structure of the histone acetyltransferase Hpa2: A tetrameric member of the Gcn5-related *N*-acetyltransferase superfamily. J Mol Biol 294:1311–1325.

Badger J, Sauder JM, Adams JM, Antonysamy S, Bain K, Bergseid MG, Buchanan SG, Buchanan MD, Batiyenko Y, Christopher JA, Emtage S, Eroshkina A, Feil I, Furlong EB, Gajiwala KS, Gao X, He D, Hendle J, Huber A, Hoda K, Kearins P, Kissinger C, Laubert B, Lewis HA, Lin J, Loomis K, Lorimer D, Louie G, Maletic M, Marsh CD, Miller I, Molinari J, Muller-Dieckmann HJ, Newman JM, Noland BW, Pagarigan B, Park F, Peat TS, Post KW, Radojicic S, Ramos A, Romero R, Rutter ME, Sanderson WE, Schwinn KD, Tresser J, Winhoven J, Wright TA, Wu L, Xu J, Harris TJ. 2005. Structural analysis of a set of proteins resulting from a bacterial genomics project. Proteins Struct Funct Bioinf 60:787–796.

Casey GP, Ingledew WM. 1986. Ethanol tolerance in yeasts. Crit Rev Microbiol 13:219–280.

Chou PY, Fasman GD. 1978. Prediction of the secondary structure of proteins from their amino acid sequence. Adv Enzymol 47:45–148.

Costa V, Amorim MA, Reis E, Quintanilha A, Moradas-Ferreira P. 1997. Mitochondrial superoxide dismutase is essential for ethanol tolerance of *Saccharomyces cerevisiae* in the post-diauxic phase. Microbiology 143:1649–1656.

Du X, Takagi H. 2005. N-Acetyltransferase Mpr1 conferred freeze tolerance in Saccharomyces cerevisiae by reducing reactive oxygen species. J Biochem 138:391–397.

Du X, Takagi H. 2007. -Acetyltransferase Mpr1 cpnfers ethanol tolerance on Saccharomyces serevisiae by reducing reactive oxygen species. Appl Microbiol Biotechnol 75:1343–1351.

Dutnall RN, Tafrov ST, Sternglanz R, Ramakrishnan V. 1998. Structure of the histone acetyltransferase Hat1: A paradigm for the GCN5-related N-acetyltransferase superfamily. Cell 94:427–438.

Dyda F, Klein DC, Hickman AB. 2000. GCN5-related N-acetyltransferases: A structural overview. Annu Rev Biophys Biomol Struct 29:81–103.

Estell DA, Graycar TP, Wells JA. 1985. Engineering an enzyme by site-directed mutagenesis to be resistant to chemical oxidation. J Biol Chem 260:6518–6521.

Fowden L. 1956. Azetidine-2-carboxylic acid: A new cyclic imono acid occurring in plants. Biochem J 64:323–332.

Hickman AB, Namboodiri MAA, Klein DC, Dyda F. 1999. The structural basis of ordered substrate binding by serotonin *N*-acetyltransferase: Enzyme complex at 1.8 A resolution with a bisubstrate analog. Cell 97:361–369.

Ho SN, Hunt HD, Horton RM, Pullen JK, Pease LR. 1989. Site-directed mutagenesis by overlap extension using the polymerase chain reaction. Gene 77:51–59.

Kimura Y, Nakamori S, Takagi H. 2002. Polymorphism of the *MPR1* gene required for toxic proline analogue resistance in the *Saccharomyces cerevisiae* complex species. Yeast 19:1437–1445.

Kotani T, Takagi H. 2008. Identification of amino acid residues essential for the yeast *N*-acetyltransferase Mpr1 activity by site-directed mutagenesis. FEMS Yeast Res 8:607–614.

Lu L, Berkey KA, Casero RAJ. 1996. RGFGIGS is an amino acid sequence required for acetyl coenzyme A binding and activity of human spermidine/spermine N1acetyltransferase. J Biol Chem 271:18920–18924.

Miyazaki-Imamura C, Oohira K, Kitagawa R, Nakano K, Yamane T, Takahashi H. 2003. Improvement of H_2O_2 stability of manganese peroxidase by combinatorial mutagenesis and high-throughput screening using in vitro expression with protein disulfide isomerase. Protein Eng 16:423–428.

Neuwald AF, Landsman D. 1997. GCN5-related histone *N*-acetyltransferases belong to a diverse superfamily that includes the yeast SPT10 protein. Trends Biochem Sci 22:154–155.

Nomura M, Takagi H. 2004. Role of the yeast acetyltransferase Mpr1 in oxidative stress: Regulation of oxygen reactive species caused by a toxic proline catabolism intermediate. Proc Natl Acad Sci USA 101:12616–12621.

Nomura M, Nakamori S, Takagi H. 2003. Characterization of novel acetyltransferases found in budding and fission yeasts that detoxify a proline analogue, azetidine-2-carboxylic acid. J Biochem 133:67–74.

Peneff C, Mengin-Lecreulx D, Bourne Y. 2001. The crystal structures of apo and complexed *Saccharomyces cerevisiae* GNA1 shed light on the catalytic mechanism of an amino-sugar *N*-acetyltransferase. J Biol Chem 276:16328–16334.

Peterson PJ, Fowden L. 1963. Different specificities of proline-activating enzymes from some plant species. Nature 200:148–151.

Piper PW. 1995. The heat shock and ethanol stress responses of yeast exhibit extensive similarity and functional overlap. FEMS Microbiol Lett 134: 121–127.

Poux AN, Cebrat M, Kim CM, Cole PA, Marmorstein R. 2002. Structure of the GCN5 histone acetyltransferase bound to a bisubstrate inhibitor. Proc Natl Acad Sci USA 99:14065–14070.

Royall JA, Ischiropoulos H. 1993. Evaluation of 2',7'-dichlorofluorescin and dihydrorhodamine 123 as fluorescent probes for intracellular H_2O_2 in cultured endothelial cells. Arch Biochem Biophys 302:348–355.

Sambrook J, Russell DW. 2001. Molecular cloning: A laboratory manual, 3rd edn. New York: Cold Spring Harbor Laboratory Press, Cold Spring Harbor.

Shichiri M, Hoshikawa C, Nakamori S, Takagi H. 2001. A novel acetyltransferase found in *Saccharomyces cerevisiae* sigma1278b that detoxifies a proline analogue, azetidine-2-carboxylic acid. J Biol Chem 276: 41998–42002.

Takagi H, Shichiri M, Takemura M, Mohri M, Nakamori S. 2000. Saccharomyces cerevisiae sigma1278b has novel genes of the N-acetyltransferase superfamily required for L-proline analogue resistance. J Bacteriol 182:4249–4256.

Tsuchiya M, Suematsu M. 1994. In vivo visualization of oxygen radical-dependent photoemission. Methods Enzymol 233:128–140.

Vetting MW, Hegde SS, Javid-Majd F, Blanchard JS, Roderick SL. 2002. Aminoglycoside 2'-*N*-acetyltransferase from *Mycobacterium tuberculosis* in complex with coenzyme A and aminoglycoside substrates. Nat Struct Biol 9:653–658.

Vetting MW, de Carvalho LPS, Yu M, Hegde SS, Magnet S, Roderick SL, Blanchard JS. 2005. Structure and functions of the GNAT superfamily of acetyltransferases. Arch Biochem Biophys 433:212–226.

Wolf E, Vassilev A, Makino Y, Sali A, Nakatani Y, Burley SK. 1998. Crystal structure of a GCN5-related N-acetyltransferase: Serratia marcescens aminoglycoside 3-N-acetyltransferase. Cell 24:439–449.

Wolf E, Angelis JD, Khalil EM, Cole PA, Burley SK. 2002. X-ray crystallographic studies of serotonin N-acetyltransferase catalysis and inhibition. J Mol Biol 317:215–224.

Wu H, Zheng X, Araki Y, Sahara H, Takagi H, Shimoi H. 2006. Global gene expression analysis of yeast cells during sake brewing. Appl Environ Microbiol 72:7353–7358.